

ON THE DETECTION OF VISUAL EVOKED RESPONSES BY USING MULTIPLE COHERENCE

A. M. F. L. Miranda de Sá IEEE member¹, L. B. Felix¹

¹Department of Electricity, Federal Institution of Higher Education of São João del Rei, MG, Brazil

Abstract—The coherence between the stimulation signal and the EEG has been used in the detection of evoked responses. However, the detector's performance depends on both the signal-to-noise ratio of the responses and the number of data segments used in the coherence estimation. Recently, the multiple coherence between the stimulation signal and the EEG has been suggested as a way of improving such detection. In this work such methodology is further investigated using Monte Carlo simulations, and the effectiveness of the method is illustrated on data recorded from 12 young normal subjects during rhythmic photic stimulation.

Keywords—EEG, photic stimulation, detection of responses, coherence, multiple coherence, Monte Carlo simulations

I. INTRODUCTION

The coherence between the stimulation signal and the EEG has been proposed as a way of detecting evoked responses embedded in the background EEG [1]. Thus, the detection task is achieved by comparing the estimated coherence with a threshold, which is obtained based on its well known sampling distribution under the null hypothesis of zero coherence (absence of evoked responses). The main advantage claimed for the technique lies on the fact that the detector is very robust, since the threshold is independent of both the shape of the response and the signal-to-noise ratio (SNR). Thus, the probability of mistakenly detecting a response (probability of false alarm) will be constant and equal to the significance level of the test. In addition, for the case of periodic, deterministic stimulation, coherence may be estimated using only the EEG signal [1], which simplifies its estimation as well as reduces random errors due to noise in data acquisition. In order to evaluate the coherence-based detectors' performance, the sampling distribution of coherence between one random and one periodic signal was derived in [2] with the aim of obtaining its confidence limits and the probability of detecting a response (PD) if such is present. The latter is shown in Fig. 1 for different SNR-values (in dB) and number of segments used in coherence estimation (M). As it can be seen, for a given SNR, the detection can only be improved by increasing M , which results in a larger stretch of EEG signal to be processed. This may constitute a serious limitation for low SNR-values, since a suitable number of segments could become large, leading to a whole data length greater than the period during the which the EEG may be considered stationary. Furthermore, in clinical applications of evoked responses such as in monitoring surgeries, one is often interest in avoiding injuries in the nervous fibbers due to surgical procedures, and therefore in detecting responses as fast as possible.

Recently, the use of multiple coherence between the stimulation and two EEG signals has been proposed as an alternative to improve the detection rate without increasing the number of segments used [3]. In the present work such methodology is further investigated with Monte Carlo simulations and applied to the EEG of 12 normal subjects during photic stimulation.

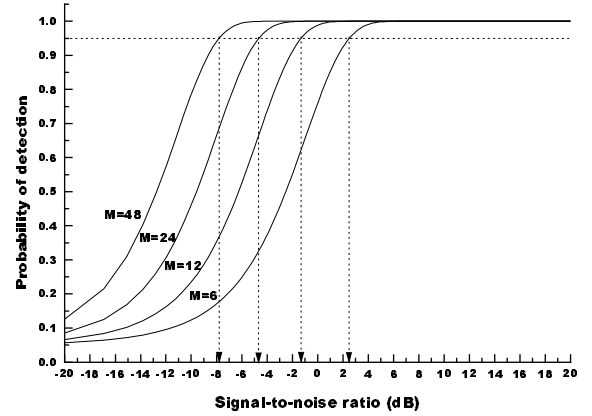


Figure 1 – Curves for the probability of detection (PD) of responses using the coherence between the stimulation signal and the EEG as a function of the signal-to-noise ratio (SNR) and for different number of windows used in the estimation ($M=6, 12, 24$ and 48). SNR-values for which PD is equal to 0.95 indicated by arrows.

II. COHERENCE BETWEEN RANDOM SIGNALS AND A PERIODICAL ONE

A. Univariate Case - $\hat{\kappa}_y^2(f)$

The coherence estimate between two finite length record, discrete-time signals $x[k]$ and $y[k]$, with the first being a periodic, deterministic signal and the latter, a random one may be obtained using the well known approach of dividing the signals into M segments as [3]:

$$\hat{\kappa}_y^2(f) = \frac{\left| \sum_{i=1}^M Y_i(f) \right|^2}{M \sum_{i=1}^M |Y_i(f)|^2}, \quad (1)$$

where “ \wedge ” superscript indicates estimation, and $Y_i(f)$ is the T -length Fourier transform of the i^{th} windowed data segment

Report Documentation Page

| | | |
|--|--|--|
| Report Date 25 Oct 2001 | Report Type N/A | Dates Covered (from... to) - |
| Title and Subtitle On The Detection of Visual Evoked Responses by Using Multiple Coherence | | Contract Number |
| | | Grant Number |
| | | Program Element Number |
| Author(s) | Project Number | |
| | Task Number | |
| | Work Unit Number | |
| Performing Organization Name(s) and Address(es) Department of Electricity Federal Institute of Higher Education of Sao Joao del Rei, MG, Brazil | | Performing Organization Report Number |
| Sponsoring/Monitoring Agency Name(s) and Address(es) US Army Research, Development & Standardization Group (UK) PSC 802 Box 15 FPO AE 09499-1500 | | Sponsor/Monitor's Acronym(s) |
| | | Sponsor/Monitor's Report Number(s) |
| Distribution/Availability Statement Approved for public release, distribution unlimited | | |
| Supplementary Notes Papers from 23rd Annual International Conference of the IEEE Engineering in Medicine and Biology Society, October 25-28, 2001, held in Istanbul, Turkey. See also ADM001351 for entire conference on cd-rom. | | |
| Abstract | | |
| Subject Terms | | |
| Report Classification unclassified | Classification of this page unclassified | |
| Classification of Abstract unclassified | Limitation of Abstract UU | |
| Number of Pages 4 | | |

of $y[k]$. Under the hypothesis of presence of responses (H_1), the sampling distribution of $\hat{\kappa}_y^2(f)$ can be obtained using the results of [4] and some further manipulations as [2]:

$$(M-1) \frac{\hat{\kappa}_y^2(f)}{1-\hat{\kappa}_y^2(f)} \sim F'_{2,2(M-1)} \left(2M \frac{\kappa_y^2(f)}{1-\kappa_y^2(f)} \right), \quad (2)$$

where “ \sim ” means “is distributed as” and $F'_{2,2(M-1)}(\lambda)$ is the noncentral F-distribution [5] with 2 and $2(M-1)$ degrees of freedom and the non-centrality parameter λ given in brackets as a function of the true value of $\kappa_y^2(f)$. For the null-hypothesis (H_0) of no response, the right hand side of (2) reduces to the (central) F distribution with 2 and $2(M-1)$ degrees of freedom, since $\kappa_y^2(f)=0$ for this particular case. The probability of detecting a response (PD) can be obtained as a function of M and $\kappa_y^2(f)$ by evaluating the integral of the probability density function of (2) from the critical value of the central F distribution (under H_0) to infinite. In Fig. 1, PD is plotted for different values of windows ($M=6, 12, 24$ and 48) and signal-to-noise ratio (SNR), which is given in dB as a function of $\kappa_y^2(f)$, as [2]:

$$(SNR)_{dB} = 10 \log(SNR) = 10 \log \left(\frac{\kappa_y^2(f)}{1-\kappa_y^2(f)} \right). \quad (3)$$

B. Two-variate case - $\hat{\kappa}_{y_2 y_1}^2(f)$

The multiple coherence expression of a periodic, deterministic signal $x[k]$, considering $y_1[k]$ and $y_2[k]$ has been derived in [3] as a particular case of the general expression given in [6] as:

$$\hat{\kappa}_{y_2 y_1}^2(f) = 1 - [1 - \hat{\kappa}_{y_1}^2(f)] \cdot [1 - \hat{\kappa}_{y_2 y_1}^2(f)], \quad (4)$$

where

$$\hat{\kappa}_{y_2 y_1}^2 = \hat{\kappa}_{y_2}^2 \cdot \frac{[1 - \text{Re}(\hat{\vartheta})]^2 + [\text{Im}(\hat{\vartheta})]^2}{[1 - \hat{\kappa}_{y_2 y_1}^2(f)] \cdot [1 - \hat{\kappa}_{y_1}^2(f)]}, \quad (5)$$

with

$$\hat{\vartheta} = \frac{\sum_{i=1}^M Y_{2i}^*(f) \cdot Y_{1i}(f) \cdot \sum_{i=1}^M Y_{1i}^*(f)}{\sum_{i=1}^M |Y_{1i}(f)|^2 \cdot \sum_{i=1}^M Y_{2i}^*(f)}. \quad (6)$$

III. SIMULATION STUDIES

Based on the model of Fig. 2, critical values of $\hat{\kappa}_{y_2 y_1}^2(f)$ where found with simulation in [3] from the

percentiles of distribution obtained by setting $H_1(f)=H_2(f)=0$, which leads $y_1[k]$ and $y_2[k]$ to be zero mean, uncorrelated Gaussian signals. This corresponds to the null hypothesis of lack of evoked responses in both signals. The alternative hypothesis may be investigated according to the following relationships [2] for the i^{th} -window Fourier Transform of $y_1[k]$ and $y_2[k]$, which are related to the theoretical values of $\hat{\kappa}_{y_1}^2(f)$ and $\hat{\kappa}_{y_2}^2(f)$ as:

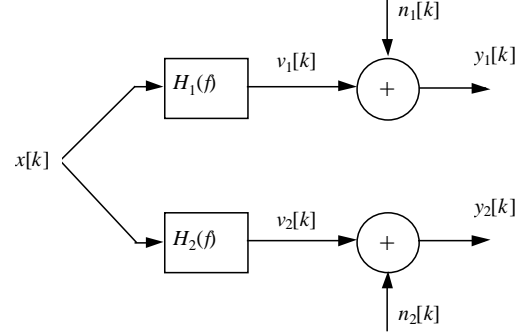


Figure 2 – Model for the EEG with an additive stimulus response. The stimuli are represented as the pulse train $x[k] \Leftrightarrow X(f)$; $v_1[k] \Leftrightarrow H_1(f)X(f)$ and $v_2[k] \Leftrightarrow H_2(f)X(f)$ are the deterministic stimulus responses; $n_1[k] \Leftrightarrow N_1(f)$ and $n_2[k] \Leftrightarrow N_2(f)$ are zero-mean, Gaussian signals with variance $\sigma_{n_1}^2$ and $\sigma_{n_2}^2$, representing the background EEG, independent of the stimuli. Finally, $y_1[k] \Leftrightarrow Y_1(f)$ and $y_2[k] \Leftrightarrow Y_2(f)$ are the measured EEG at two distinct regions.

$$Y_{1i}(f) = \sqrt{\frac{2\sigma_{f1}^2 \cdot \kappa_{y1}^2(f)}{1-\kappa_{y1}^2(f)}} + N_{1i}(f) \\ Y_{2i}(f) = \sqrt{\frac{2\sigma_{f2}^2 \cdot \kappa_{y2}^2(f)}{1-\kappa_{y2}^2(f)}} + N_{2i}(f) \quad , i = 1, 2, \dots, M \quad (7)$$

where $N_{1i}(f)$ and $N_{2i}(f)$ are, respectively, the i^{th} -window Fourier Transform of $n_1[k]$ and $n_2[k]$, whose real and imaginary parts are zero-mean, Gaussian distributed with variance σ_{f1}^2 and σ_{f2}^2 . The detection rate with $\hat{\kappa}_{y_2 y_1}^2(f)$ was experimentally obtained in [3] by generating a population of $Y_{1i}(f)$ and $Y_{2i}(f)$ -values according to (7) and counting the cases in which $\hat{\kappa}_{y_2 y_1}^2(f)$ was greater than its critical value.

This was done for different values of M and SNR, which are related to $\kappa_{y1}^2(f)$ and $\kappa_{y2}^2(f)$ according to (3). However, in this work such values were assumed to be equal in both signals in order to allow a comparison to the probability of detection (PD) with $\hat{\kappa}_y^2(f)$ (Fig. 1). The general case of different values of SNR for $y_1[k]$ and $y_2[k]$ is now investigated for $M=12$ and $N=10^3$ iterations using the same methodology as in [3], leading to the 3-D plot shown in Fig. 3.

As it can be seen, for a fixed SNR-value in $y_1[k]$, an infinite number of PD-values may be found, depending on the SNR in $y_2[k]$. On the other hand, if we fix the probability of

detection, the infinite pairs of SNR in $y_1[k]$ and in $y_2[k]$ (SNR_1 and SNR_2) leading to the same PD may be found as the contour maps in the xy-plane of Fig.3. Such information is very important in order to obtain the minimum SNR in $y_2[k]$ that improves the detection rate when using both $y_1[k]$ and $y_2[k]$ (detection with $\hat{\kappa}_{y_2y_1}^2(f)$) in comparison to that one using only one signal (detection with $\hat{\kappa}_y^2(f)$).

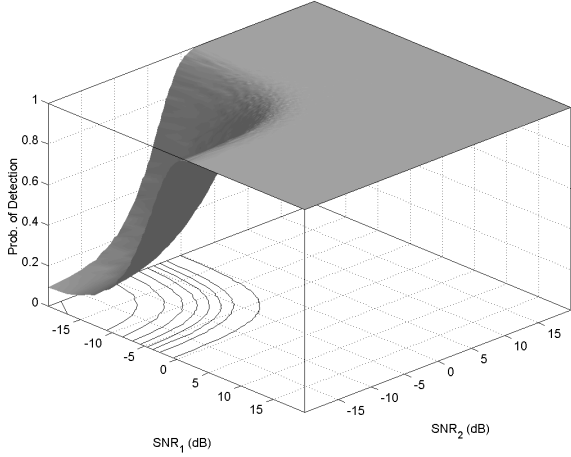


Figure 3 - Probability of detection with $\hat{\kappa}_{y_2y_1}^2(f)$ as a function of SNR-values of $y_1[k]$ and $y_2[k]$. Contour maps are shown in the xy-plane.

In Fig. 4, the case of PD=0.95 is taken as an example. If only one signal is used in the detection with coherence, a PD of 0.95 is expected for a signal-to-noise ratio of -1.2 dB with $M=12$ (Fig. 1). Setting this value of SNR for $y_1[k]$ on the contour curve of Fig. 4, a corresponding SNR of about -10 dB is found for $y_2[k]$. Thus, for SNR-values greater than this one, an improvement in the detection is expected, since the intersection between the horizontal and vertical dotted lines would lie on a contour curve above that one for PD=0.95. On the other hand, for a SNR in $y_2[k]$ lower than this threshold, a smaller detection rate is expected when using both signals.

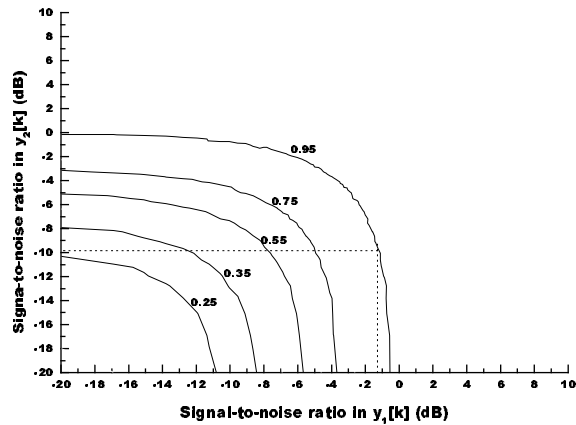


Figure 4 - Contour plot of the PD-values from Fig. 3 with PD=0.25, 0.35, 0.55, 0.75, and 0.95.

The particular case when the SNR is equal in both signals corresponds to the intersection between the bisector-plane and the 3-D curve of Fig. 3, and is shown in Fig. 5, together with the probability of detection using $\hat{\kappa}_y^2(f)$. As it can be noted, PD is always greater when using $\hat{\kappa}_{y_2y_1}^2(f)$ in comparison with the univariate case.

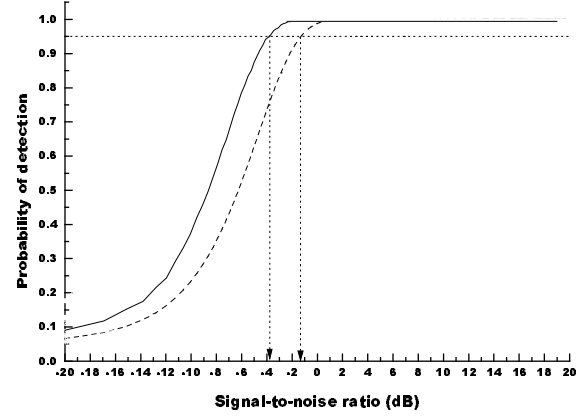


Figure 5 - Probability of detecting a response with $\hat{\kappa}_{y_2y_1}^2(f)$ for the case when signals $y_1[k]$ and $y_2[k]$ have the same SNR for $M=12$ (continuous line). PD with $\hat{\kappa}_y^2(f)$ is also shown in dotted line to allow comparison.

IV. APPLICATION TO EEG DURING PHOTIC STIMULATION

In order to compare the performance of $\hat{\kappa}_{y_2y_1}^2(f)$ to that of $\hat{\kappa}_y^2(f)$, the EEG of 12 normal young subjects (age range: 9 – 17 years) was recorded at derivations O_1 and O_2 (reference: ipsilateral earlobe) over a period of 24 seconds during intermittent photic (flash) stimulation at 10 Hz. The signals were digitised at 256 Hz, and the coherences calculated following (1) for O_1 and (4)-(6) for both derivations, using $M=12$ epochs each of 2 second duration and applying a rectangular window. A typical result is displayed in Fig. 6.

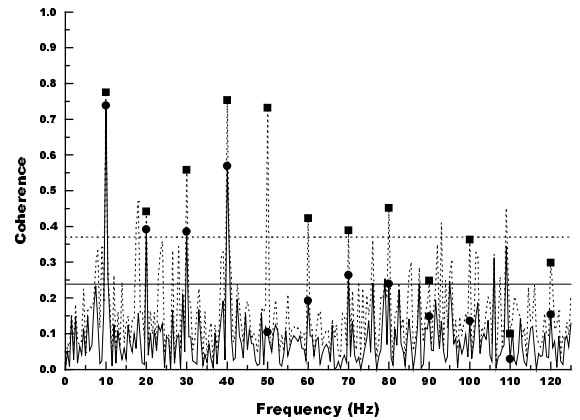


Figure 6 - $\hat{\kappa}_{y_2y_1}^2(f)$ (dotted line, harmonics of the stimulation frequency indicated by squares) and $\hat{\kappa}_y^2(f)$ calculated for O_1 from subject #1 (continuous line, harmonics of the stimulation frequency indicated by circles). Critical values are shown in horizontal lines.

Regarding the harmonics of the stimulation frequency for this example, it can be noted that the number of cases for which $\hat{\kappa}_{y2y1}^2(f)$ lie above its critical value is significantly greater than that one for $\hat{\kappa}_y^2(f)$. This reflects in a higher detection rate for the first estimate (75%) in comparison to the latter (50%). Such results are in agreement with Fig. 5. However, for some other subjects, the detection rate-values are not compatible with Fig. 5, as in Fig. 7. In this case, a detection rate of 83% is found with $\hat{\kappa}_{y2y1}^2(f)$, while 75% of responses were detected with $\hat{\kappa}_y^2(f)$. This case must be interpreted as different SNR-values in the EEG derivations.

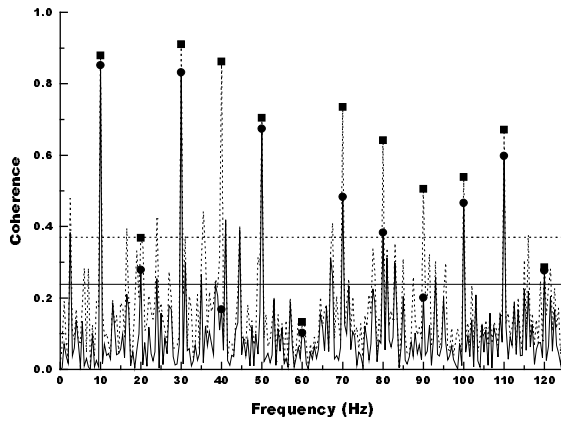


Figure 7 - $\hat{\kappa}_{y2y1}^2(f)$ (dotted line and harmonics of the stimulation frequency indicated by squares) and $\hat{\kappa}_y^2(f)$ calculated for O_1 from subject #2 (continuous line and harmonics of the stimulation frequency indicated by circles). Critical values are shown in horizontal lines.

In spite of the relationship involving the SNR in O_1 and O_2 , the performance of $\hat{\kappa}_{y2y1}^2(f)$ was always superior to that of $\hat{\kappa}_y^2(f)$, as evident in the histogram of the difference between the number of detections with both estimates (Fig. 8).

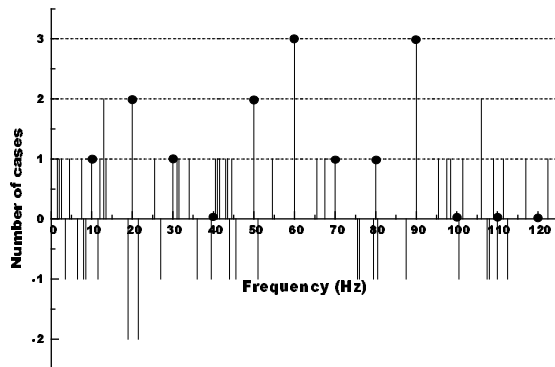


Figure 8 – Difference between the number of detection with $\hat{\kappa}_{y2y1}^2(f)$ and $\hat{\kappa}_y^2(f)$ as a function of frequency. Negative numbers correspond to frequencies for which the detection with the latter was greater than that with the first. Stimulation frequency and harmonics indicated by circles.

V. CONCLUSION

In [3], a technique for detecting evoked responses was developed based on the extension to the multivariate case of coherence between the stimulation signal and EEG. Thus, instead of using the EEG collected at a unique region, it was proposed the estimation using two EEG derivations. This multiple coherence ($\hat{\kappa}_{y2y1}^2(f)$) is also independent of the stimulation signal (see (4)-(6)). However, the probability of detecting a response (PD) was obtained in such work assuming equal values in the signal-to-noise ratio (SNR) of both signals. This was done in order to allow a direct comparison to the simple coherence as in Fig. 5, and may be justified based on the well-known inter-hemispheric symmetry of the visual evoked responses [7].

In the present work the general case was investigated leading to the 3-D curve of Fig. 3, whose contour maps allow obtaining the minimum SNR in the second signal that improves the detectors' performance. For the case of PD=0.95 and $M=12$ segments, such threshold is of -10 dB, which is much smaller than the SNR necessary for the same PD using only one signal (-1.2 dB). Thus, for closer SNR-values, a higher detection rate is expected with $\hat{\kappa}_{y2y1}^2(f)$.

The results with EEG signals confirm the better performance of $\hat{\kappa}_{y2y1}^2(f)$ and suggest its use in order to improve the detection of evoked responses.

ACKNOWLEDGMENT

The authors gratefully acknowledge the assistance from Dr. V. Lazarev and the Laboratory of Clinical Neurophysiology of the Instituto Fernandes Figueira, Rio de Janeiro, in data collection. This work received financial support of the Fundação Tiradentes – FUNTIR/FUNREI, Brazil.

REFERENCES

- [1] R.A. Dobie and M.J. Wilson, "Analysis of auditory evoked potentials by magnitude-squared coherence", *Ear and Hearing*, vol. 10, no. 1, pp. 2-13, February 1989.
- [2] A.M.F.L. Miranda de Sá, D.M. Simpson, and A.F.C. Infantesi, "Coherence between one random and one periodic signal – application to the EEG during sensory stimulation". Digest of Papers of the 2000 World Congress on Medical Physics and Biomedical Engineering and the Proceedings of the 22nd Annual International Conference of the IEEE Engineering in Medicine and Biology Society.
- [3] A.M.F.L. Miranda de Sá, *Desenvolvimento de Técnicas para o Estudo da Coerência no EEG durante Foto-Estimulação Intermitente*, D.Sc. Thesis, Biomedical Engineering Program - COPPE, Federal University of Rio de Janeiro, Brazil.
- [4] D.R. Brillinger, *Time Series Analysis and Theory*, New York: Holt, Rinehart and Winston 1975, pp.190.
- [5] S.M. Kay, *Fundamentals of Statistical Signal Processing volume II detection theory*, New Jersey: Prentice-Hall, 1998, pp.29.
- [6] G.M. Jenkins and D.G. Watts, *Spectral Analysis and its Applications*, Oakland: Holden-Day, 1968, pp. 488-489.
- [7] B.M. Coull and T.A. Peddley, "Intermittent photic stimulation. Clinical usefulness of non-convulsive responses". *Electroenc. Clin. Neurophysiol.* vol. 44, pp. 353-363, 1978.